Flow Turbulence Combust (2007) 79:41–53
DOI 10.1007/s10494-006-9063-1

# Impact of Turbulent Flow and Mean Mixture Fraction Results on Mixing Model Behavior in Transported Scalar PDF Simulations of Turbulent Non-premixed Bluff Body Flames

**Bart Merci · Bertrand Naud · Dirk Roekaerts**

Received: 24 July 2006 / Accepted: 24 November 2006 /
Published online: 28 February 2007


**Abstract** Numerical simulation results are presented for three turbulent jet diffusion flames, stabilized behind a bluff body (Sydney Flames HM1-3). Interaction between turbulence and combustion is modeled with the transported joint-scalar PDF approach. The focus of the study is on the impact of the quality of simulation results in physical space on the behavior of two micro-mixing models in composition space: the Euclidean Minimum Spanning Tree ('EMST') model and the modified Curl coalescence dispersion ('CD') model. Profiles of conditional means and variances of thermo-chemical quantities, conditioned on the mixture fraction, are discussed in the recirculation region and in the neck zone behind. The impact of the flow and mixing fields in physical space on the mixing model behavior in composition space is strong for the CD model and increases as the turbulence – chemistry interaction becomes stronger. The EMST conditional profiles, on the contrary, are hardly affected.

**Key words** transported scalar PDF · micro-mixing models · turbulent non-premixed flames · bluff body

B. Merci (✉)
Department of Flow, Heat and Combustion Mechanics, Ghent University – UGent,
Sint-Pietersnieuwstraat 41, 9000 Ghent, Belgium
e-mail: Bart.Merci@UGent.be

B. Merci
Postdoctoral Fellow of the Fund of Scientific Research – Flanders (Belgium)
(FWO-Vlaanderen), Brussels, Belgium

B. Naud
CIEMAT, Madrid, Spain

D. Roekaerts
Department of Multi-scale Physics, Delft University of Technology, Delft, The Netherlands

**Abbreviations**

| | |
|---|---|
| CD | coalescence/dispersion |
| $C_\phi$ | micro-mixing model constant |
| $D_\mathrm{b}$ | bluff body diameter (m) |
| EMST | Euclidean Minimum Spanning Tree |
| $F$ | probability density function |
| $F$ | mass density function |
| IP | isotropization of production |
| ISAT | in situ adaptive tabulation |
| $J_{ik}$ | diffusive flux of species k in direction i (kg/(m$^2$s)) |
| $K$ | turbulent kinetic energy (m$^2$/s$^2$) |
| LRR | Launder–Reece–Rodi |
| NL | non-linear |
| PDF | probability density function |
| $R$ | radial distance (m) |
| $R_\mathrm{b}$ | bluff body radius (m) |
| SM | Reynolds stress model |
| $S_k$ | chemical source term for species k (kg/s) |
| $Sc_\mathrm{t}$ | turbulent Schmidt number (–) |
| $T$ | temperature (K) |
| TR | time scale ratio (–) |
| $U_\mathrm{I}$ | mean velocity component (m/s) |
| $x_\mathrm{I}$ | coordinate direction |
| $X$ | axial coordinate (m) |
| $Y$ | species mass fraction (–) |
| $\Gamma_\mathrm{t}$ | turbulent diffusivity (Pa s) |
| $\varepsilon$ | turbulent dissipation rate (m$^2$/s$^3$) |
| $\mu_\mathrm{t}$ | turbulent viscosity |
| $\rho$ | density (kg/m$^3$) |
| $\psi$ | composition space sample variable (–) |
| $\xi$ | mixture fraction (–) |

## 1 Introduction

The transported PDF methodology [1] provides a very useful framework for numerical simulations of turbulent flames with strong turbulence – chemistry interaction. In the current study we investigate three turbulent jet diffusion flames, stabilized behind a bluff body (Sydney flames HM1-3) [(http://www.ca.sandia.gov/TNF), 2, 3]. These flames have been target test cases in the international series of TNF workshops [http://www.ca.sandia.gov/TNF].

We apply the transported joint-scalar probability density function ('PDF') method in the RANS context. The velocity components are thus no density variables in the PDF. An important model ingredient for turbulent non-premixed flames concerns the mixing on molecular scale. We consider two widely used micro-mixing models: the modified Curl 'Coalescence Dispersion ('CD') [4] and the Euclidean Minimum Spanning Tree ('EMST') model [5, 6, (http://eccentric.mae.cornell.edu/~laniu/emst)]. In recent articles (e.g. [7–12]), differences in the micro-mixing model behavior have been investigated. As a first step, it is

common practice to make sure that the numerical predictions in physical space are as accurate as possible. This implies both mean quantities and fluctuations in the flow and mixing fields. Once this objective has been met satisfactorily, the micro-mixing behavior in composition space is investigated, using profiles of conditional (on mixture fraction) means and fluctuations and/or the underlying scatter plots. The two steps can thus be referred to as results in physical space and results in composition space. The second step is considered the most relevant in relation to the study of turbulence-chemistry interaction. In comparative studies of micro-mixing models, it is certainly viable to make sure first that the results in physical space are as accurate as possible, in order to reduce uncertainties. An extreme example is the use of DNS data [8]. In [12], we also followed this approach and reported on the differences between the micro-mixing models due to their intrinsic properties, as they become visible in the results in physical space and composition space. We therefore optimized the RANS turbulence model in [12] in order to obtain as good agreement with experimental data as possible in physical space.

However, it is also important to know the sensitivity of the micro-mixing model behavior in composition space with respect to the quality of the results in physical space. This is particularly true for blind test cases, where it may be impossible to judge on the quality of the results in physical space a priori. The study of this sensitivity is the subject of the present paper. In that sense, the present work can be seen as an extension of the study reported in [12]. We stress that the aim here is not a study of the quality of the micro-mixing models in terms of agreement with experimental data. This was the subject of [12]. Rather, we show in a quantitative manner, by means of conditional profiles in mixture fraction space, the impact of the quality of the results in physical space on the results in composition space, for the two micro-mixing models mentioned.

To that purpose, we compare, for each of the two micro-mixing models, conditional profiles in composition space, resulting from the combination with the 'modified LRR-IP' Reynolds stress model ('RSM') [13], to the profiles resulting from the combination with the non-linear ('NL') k-ε model of [14], in first order formulation. Indeed, the two turbulence models lead to different results in physical space.

Finally, we remark that in [10] the impact of chemistry modeling on the micro-mixing modeling has been reported, with focus on EMST. We keep the chemistry model fixed and use the skeletal mechanism of [15]. Radiation is neglected, because inclusion of radiation only affects mean temperature and minor species [11]. It does not affect the conclusions of the present paper.

## 2 Test Case Description

A complete description of the experimental set-up is found in [http://www.ca.sandia.gov/TNF, 3]. The bluff body burner has an outer diameter $D_b$=50 mm. The central fuel jet, with diameter 3.6 mm, is separated from the co-flow air stream. Fuel and air mix to form a non-premixed turbulent flame. The flame is stabilized by mixing of hot products, air and fuel in the recirculation region behind the bluff body.

The fuel consists of 50% $H_2$ and 50% $CH_4$ by volume. The bulk jet exit velocities are: 118 m/s (HM1), 178 m/s (HM2) and 214 m/s (HM3). The co-flow air free stream mean velocity is $U_{cf}$=40 m/s for all three flames.

The simulations have been performed with Fluent, version 6.2. The numerical settings are identical to what is described in [12]. We only report the most important features here.

We use a non-uniform rectangular computational mesh of 90×100 cells. The grid inlet plane is positioned $0.2D_b$ upstream of the nozzle exit ($x$=0). The outlet is at $x=7.2D_b$. In the radial direction, the grid extends from $r$=0 to $r=3D_b$.

At the inlet boundary, a fully developed central fuel jet and a boundary layer co-flow are applied. At the outer radial boundary and the exit boundary, atmospheric static pressure is prescribed and zero radial or axial derivatives are imposed. At the adiabatic solid boundaries, no-slip conditions are applied. The turbulence models are in low-Reynolds formulation, so that calculations are performed up to the solid boundary. For the scalars, zero diffusive fluxes are imposed.

The transport equation for the mass density function is solved in a Lagrangian manner, following a large number of particles. The number of particles per cell $N_{PC}$ is $N_{PC}$=100. Statistical error is reduced by means of time averaging over the latest 100 iterations.

In Situ Adaptive Tabulation ('ISAT') [16] is applied as efficient implementation of detailed chemistry. As in [12], the ISAT error tolerance is set to $\varepsilon_{tol}=10^{-4}$.

## 3 Modeling

### 3.1 Flow field modeling

As mentioned in the introduction, two different turbulence models are applied in order to evaluate the impact of the physical space results on the micro-mixing model behavior in composition space. Since the focus of the present paper is not on the comparison of the quality of the two turbulence models, we only briefly describe their most important features.

The first is the 'modified LRR-IP' RSM. As described in [12], the major modification to the original LRR-IP model [17] is the increase of the value of model constant $c_{\varepsilon 1}$ in the dissipation rate transport equation from $c_{\varepsilon 1} = 1.44 - 1.6$, for better round jet spreading rate predictions. The value $c_{\varepsilon 1} = 1.92$ is kept.

The second turbulence model is the non-linear ('NL') k-ε model of [14]. Only the first order terms are retained. This does not affect the results, because the resulting force in the momentum equations from the higher order terms, as well as their contribution to the production of turbulent kinetic energy, are negligible. The major difference to the earlier model, used in [18], is the application of the dissipation transport equation of [19], which ensures a correct spreading rate prediction of both the planar and the round jet, without model parameter tuning. However, as is discussed below, compared to the modified LRR-IP model, this leads to less accurate predictions in physical space for the bluff body burner test cases.

Since the RSM results are in better agreement with experimental data than the NL model results, the impact of this difference on the micro-mixing model behavior can be investigated.

### 3.2 Composition field modeling

As mentioned in the introduction, we apply the skeletal scheme of [15] as detailed chemistry model. It contains 31 reactions with 16 species: $CH_4$, $O_2$, $H_2O$, $CO_2$, CO, $H_2$, H, O, OH, $HO_2$, $H_2O_2$, $CH_3$, $CH_3O$, $CH_2O$, HCO and $N_2$.

The modeled transport equation for the mass density function $F(\psi;x,t) = \langle\rho\rangle\widetilde{f}(\psi;x,t)$ is solved (with $\widetilde{f}(\psi;x,t)$ the Favre PDF):

$$\frac{\partial F}{\partial t} + \frac{\partial}{\partial x_j}\left(\widetilde{U}_j F\right) + \frac{\partial}{\partial \psi_k}\left(S_k F\right) = \frac{\partial}{\partial x_j}\left(\Gamma_t \frac{\partial \widetilde{f}}{\partial x_k}\right) + \frac{\partial}{\partial \psi_k}\left(\left\langle \frac{1}{\rho}\frac{\partial J_{i,k}}{\partial x_i}\middle|\psi\right\rangle F\right). \quad (1)$$

As explained in [11], the equation is solved in a Lagrangian manner with local time stepping. Particles reflect at solid boundaries. In the random walk model for the turbulent diffusion term, the turbulent diffusivity is defined as $\Gamma_t = \frac{\mu_t}{Sc_t}$ with constant turbulent Schmidt number $Sc_t = 0.85$, as in [12].

The micro-mixing model closes the last term on the right hand side in (1). Fox [20] gives an excellent review on 'constraints' and 'desirable properties' of micro-mixing models. In the context of the present study, the most relevant difference between the CD and EMST model is that EMST has the intrinsic 'localness principle', while CD does not. Indeed, with EMST particles only interact with neighboring particles in composition space, while with CD particles undergo jumps in composition space, by pair-wise interaction (coalescence and dispersion) in a stochastic manner.

## 4 Coalescence/Dispersion Micro-mixing Model

The results are discussed for the three flames separately. The level of turbulence – chemistry interaction increases from flame HM1 to flame HM3. We repeat that the focus is on the impact of physical space results on the micro-mixing model behavior, not on the quality of the physical space results itself. All averages are Favre averages.

### 4.1 Flame HM1

Figure 1 shows physical space results at different axial positions inside the recirculation region behind the bluff body ($x<D_b$) and in the 'neck' zone behind ($x>D_b$). Mixture fraction is determined by Bilger's formula [21]. As reported in [12], the RSM results are in reasonable agreement with the experimental data, while we now show that the quality of the NL results in physical space is less satisfactory. In order to evaluate the effect in composition space, we first examine Fig. 2, showing the ratio of a physical space time scale and the characteristic micro-mixing time scale:

$$TR = \frac{\min(\tau_{\text{conv}};\tau_{\text{diff}})}{\tau_{\text{mix}}} = \frac{\min\left(\frac{k^{3/2}/\varepsilon}{\sqrt{U^2+V^2}};\frac{k}{\varepsilon}\right)}{C_\phi^{-1}\frac{k}{\varepsilon}} = C_\phi \min\left(\frac{\sqrt{k}}{\sqrt{U^2+V^2}};1\right). \quad (2)$$

The numerator takes the minimum of the mean convection time scale and a macro-scale turbulent diffusion time scale, which is set equal to the local integral turbulent time scale. In the denominator, the characteristic micro-mixing time scale is, as usual, set equal to the local integral turbulent time scale, with proportionality factor $C_\phi$. The default value of $C_\phi$ is 2 for the CD model, while it is 1.5 for the EMST model [7]. The discussion in the present paper is independent of this model constant value choice. In [12] it is explained that

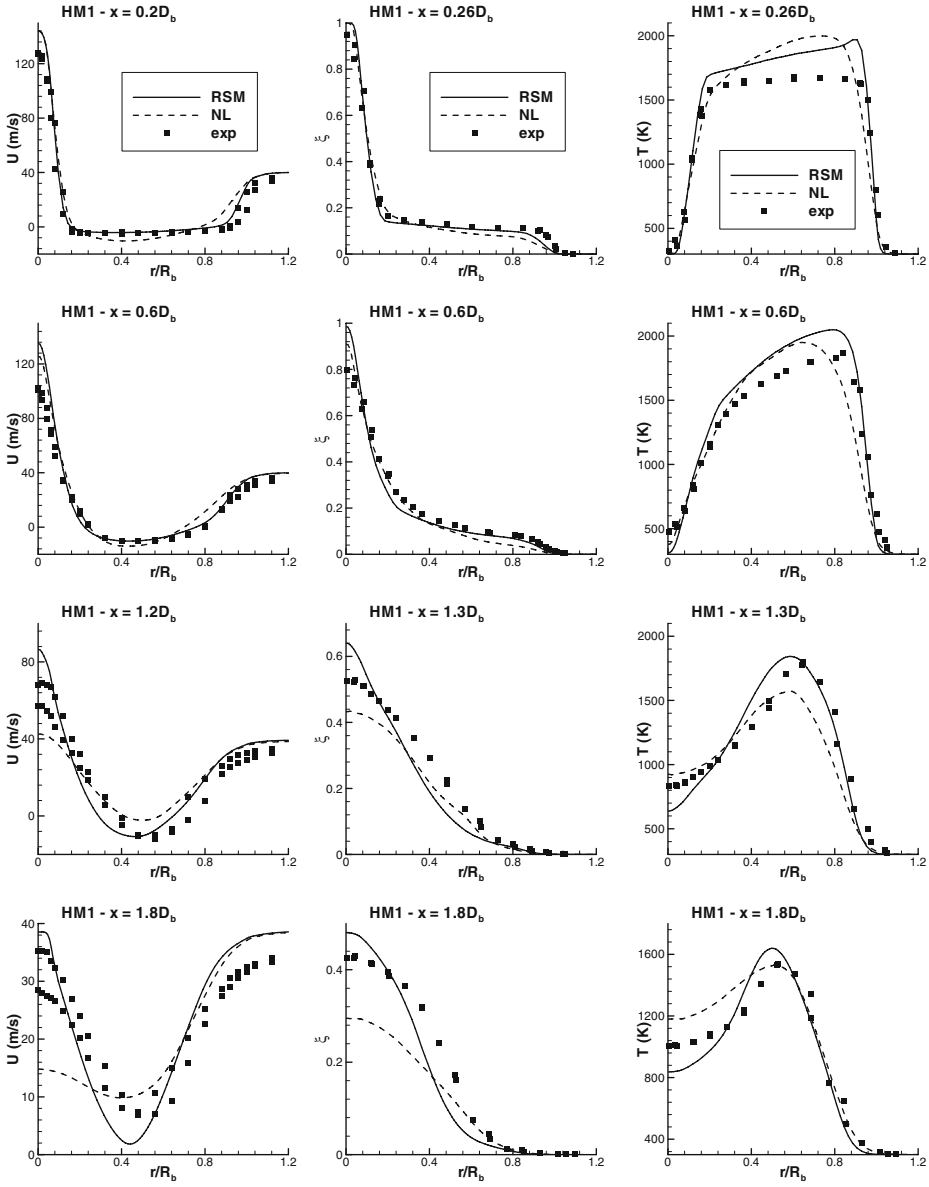


**Fig. 1** Results in physical space for flame HM1 with the CD micro-mixing model

particles receive more time to interact with other particles as ratio (2) becomes larger. Consequently, the micro-mixing model behavior can be affected when the time scale ratio is not accurately predicted. In this sense, we note the large difference between the RSM and the NL results in the neck zone ($x$=1.8$D_b$). Consequently, the particles clearly receive less time to interact with one another when the results in physical space are obtained with the NL model. We discuss now the effect hereof on the results in composition space, in terms of conditional means and fluctuations.

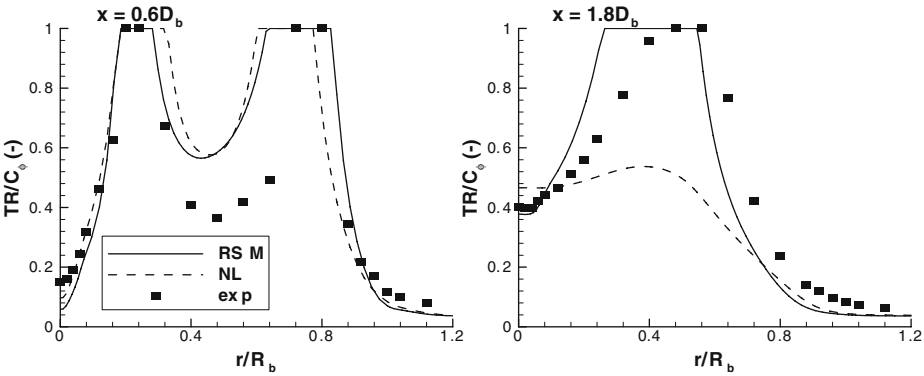


**Fig. 2** Time scale ratio (2) for flame HM1 (CD micro-mixing model)

Figure 3 gives profiles of conditional mean and fluctuation values for temperature at $x=0.6D_b$ and $x=1.8D_b$, which provide a more quantitative test than scatter plots. The values are conditioned on mixture fraction, using intervals of width 0.005. We observe relatively small differences in the recirculation region, in line with the small differences in Fig. 2. In the neck zone, we see a substantial increase in conditional fluctuations when the NL model is applied, in line with the shorter time the particles receive to interact with one another (Fig. 2). This results in lower conditional mean values. The primary observation is thus that

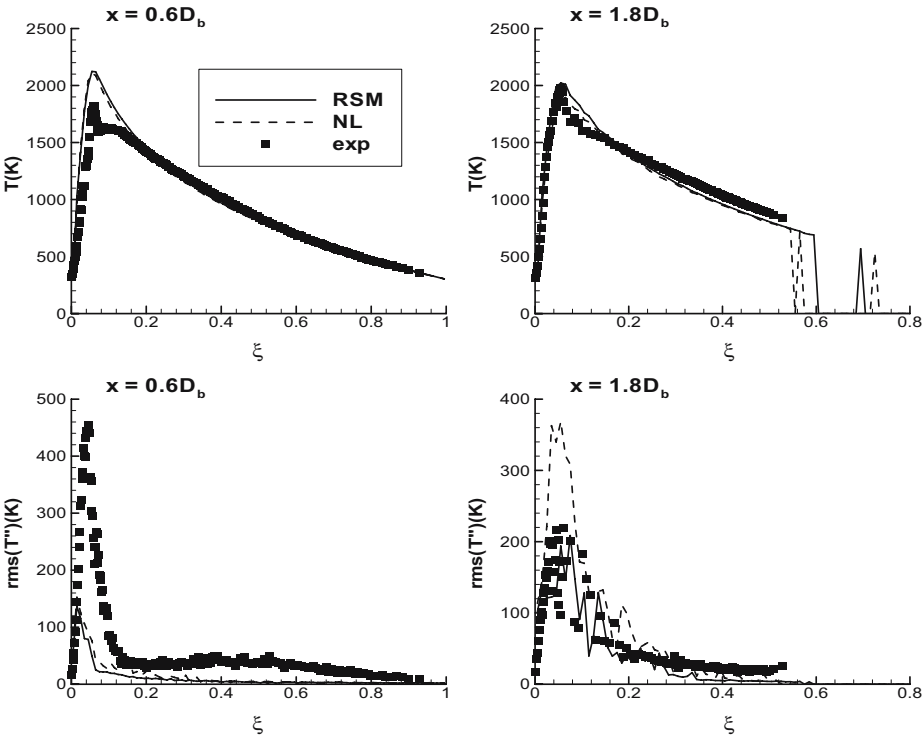


**Fig. 3** Conditional temperature profiles for flame HM1 (CD micro-mixing model)

there are clear differences between the results with RSM and NL. This reveals a strong sensitivity of the CD micro-mixing model behavior to the results in physical space. This sensitivity is due to the mentioned basic principle of the CD model: particles interact pair-wise with randomly chosen other particles in the cell. Thus, there is an a priori strong dependence on the 'instantaneous' PDF in a given cell and, as such, there is a direct influence from the quality of the physical space results on the behavior in composition space. Indeed, together with the turbulence frequency and the $C_\alpha$ model constant value, the flow and mixing fields in physical space determine this instantaneous PDF in the cell (through convection and large scale mixing), on which the micro-mixing model acts in composition space.

As a second observation, we remark that, particularly at $x=1.8D_b$, far more particles evolve towards the inert mixing line when the NL model is used, indicating a stronger tendency towards local extinction. This is seen in the higher level of conditional fluctuations and lower conditional mean temperature values.

## 4.2 Flame HM2

In [12] it is illustrated that reasonable agreement is obtained with experimental data in physical space when the RSM turbulence model is used. As for flame HM1, the quality deteriorates when the NL model is applied (not shown). Figure 4 shows the impact on the micro-mixing model behavior by means of conditional profiles. As for flame HM1, a substantial increase in conditional fluctuations is revealed when the NL model is used.

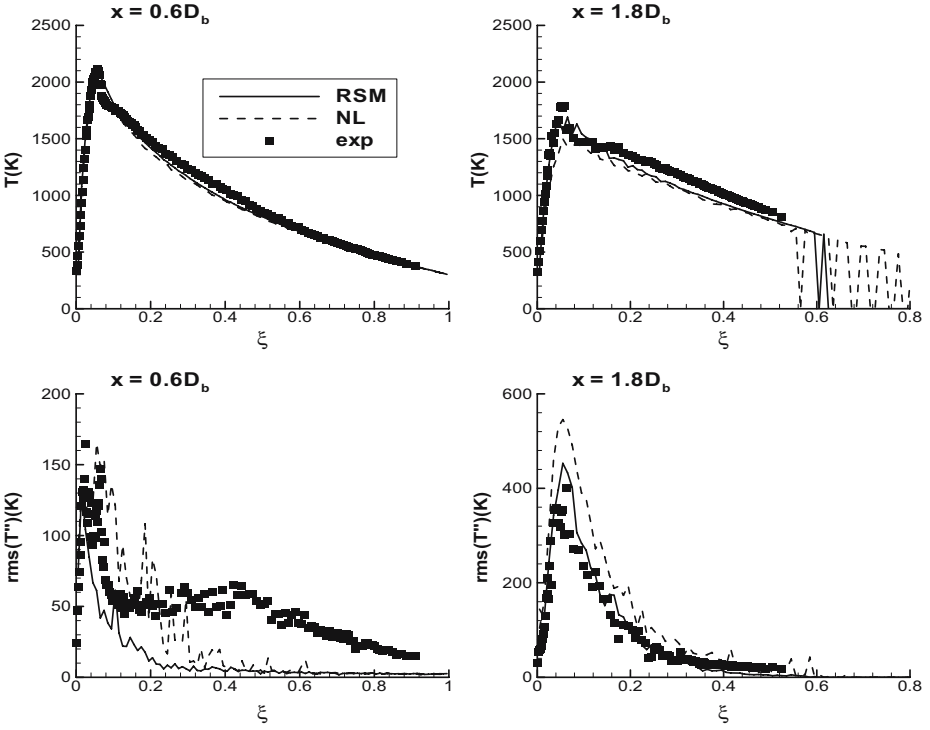


**Fig. 4** Conditional temperature profiles for flame HM2 (CD micro-mixing model)

Thus, the strong impact of the physical space results on the behavior in composition space, as observed for flame HM1 in the previous section, is confirmed for flame HM2.Also note the wider range of mixture fraction values with the NL model, in particular in the neck zone. This is due to a higher level of unconditional mixture fraction fluctuations (not shown).

### 4.3 Flame HM3

As already mentioned, this flame has the strongest turbulence – chemistry interaction in the flame series. With the NL model, a statistically stationary solution could be obtained. With the RSM on the other hand, we did not succeed with the CD micro-mixing model. We observe the following limit cycle: the 'normal' flame, that should be statistically stationary, stabilized by the bluff body, tends to extinguish and evolves to a situation where there are only hot gases immediately behind the bluff body. Due to this heat, the mixture of fuel and air ignites again and the 'normal' flame is recovered. In contrast to the experiments, however, this flame is not stable and the limit cycle, as described, is established. Consequently, we do not present results for the RSM model. The completely different behavior in physical space is a consequence of the CD micro-mixing model, because too many particles evolve towards local extinction, so that the flame becomes unstable. In Section 5 we indeed illustrate that this does not occur with the EMST micro-mixing model. Most probably the NL model does not suffer from this phenomenon because it is less sensitive to density variations than the RSM model.

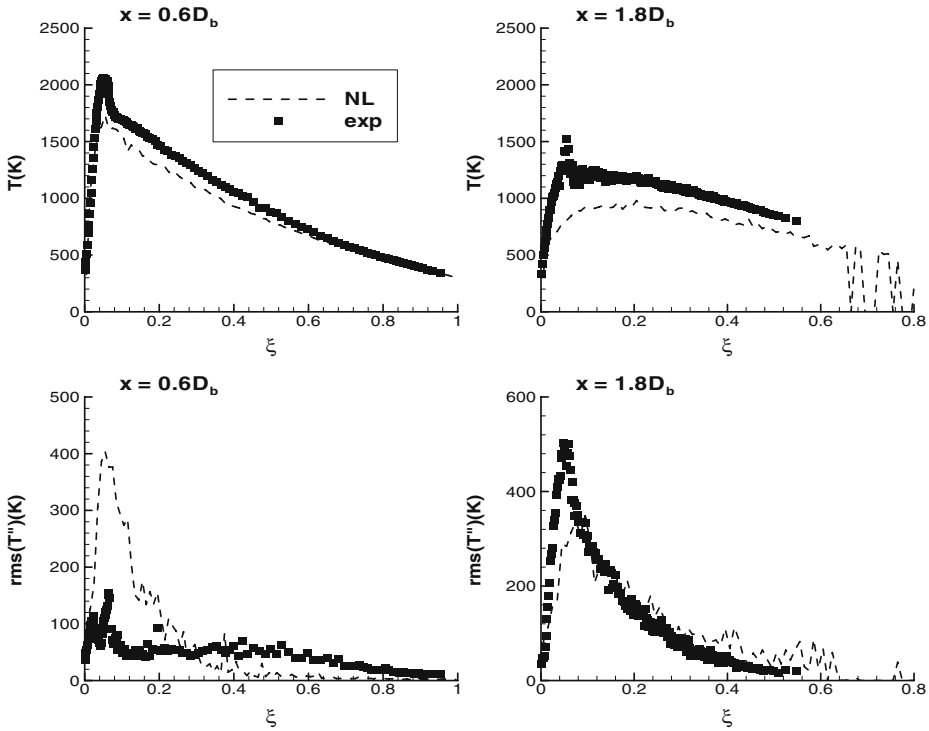


**Fig. 5** Conditional temperature profiles for flame HM3 (CD micro-mixing models; only NL gives statistically stationary solution)

Figure 5 provides conditional profiles. Too high levels of conditional fluctuations are observed in the recirculation region. This corresponds to an evolution of too many particles towards the extinction limit. In the neck zone, far too many particles are in the inert mixing zone, reflected in too low values for the conditional mean temperature. The conditional temperature fluctuations are not over-predicted, because relatively few particles are fully burning. Still, the flame does not extinguish globally.

## 5 Euclidean Minimum Spanning Tree Micro-mixing Model

With the important exception that for flame HM3 a statistically stationary solution is also found with the RSM model in combination with the EMST model, the results in physical space with EMST are almost identical as with the CD micro-mixing model, as illustrated in [12]. This implies that, for the flames under study and with the chemistry model applied, the impact of the micro-mixing model choice on the results in physical space (through the mean density) is small. We restrict ourselves again to conditional profiles from now on. We only show results for flames HM1 and HM3 (since HM2 is very similar with EMST).

Figures 6 and 7 reveal that there is very little impact of the physical space results on the level of conditional fluctuations. This is seen in the relatively small differences between the NL and SMC results. This is true, both in the recirculation region and in the neck zone.

This clearly illustrates that the EMST behavior in composition space is hardly affected by the quality of the physical space predictions. This is a direct consequence of the

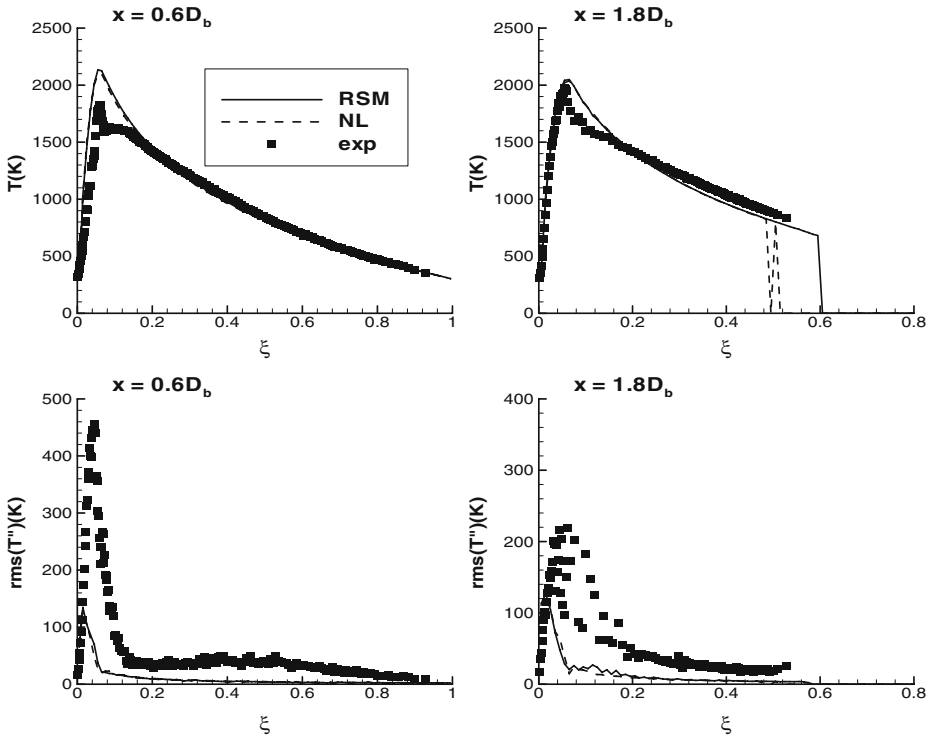


**Fig. 6** Conditional temperature profiles for flame HM1 (EMST micro-mixing model)

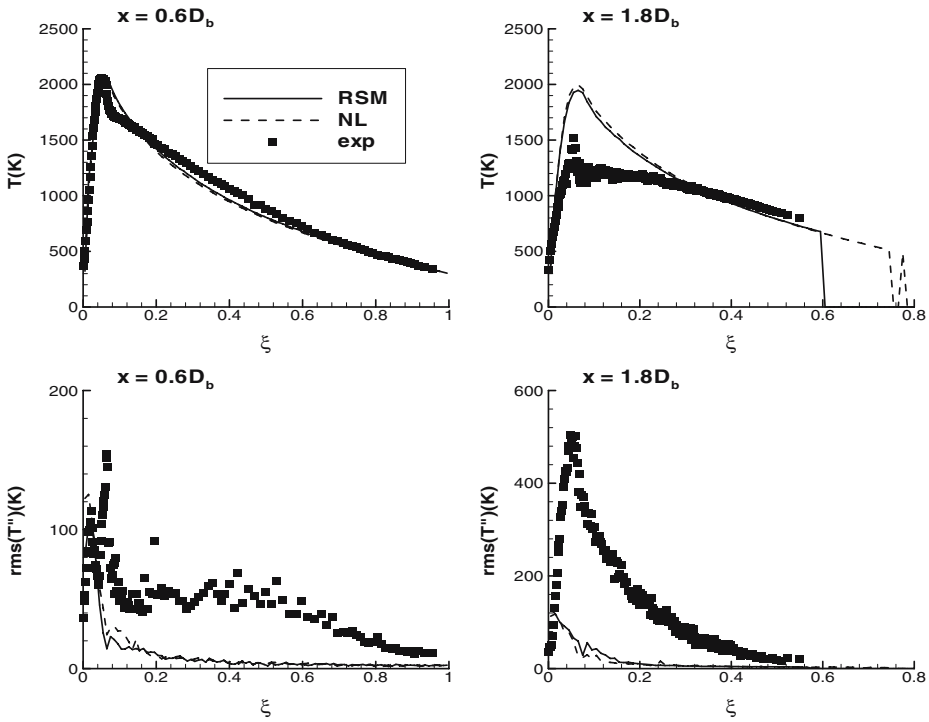


**Fig. 7** Conditional temperature profiles for flame HM3 (EMST micro-mixing model)

localness property of this micro-mixing model: particles interact mainly with neighboring particles in composition space. Thus, the impact of the quality of the flow and mixing field predictions in physical space, which still determine the input for the micro-mixing model in composition space, is less direct than for the CD model, where particles interact randomly with other particles in the same cell. As such, the behavior remains largely unaffected as long as the same fuel and oxidizer and the same chemistry model are applied. Note that, while the robustness of the EMST with respect to the quality in physical space can be interpreted as an advantage, the price to pay is an under-estimation of local extinction, as discussed in [12]. This under-prediction of local extinction becomes more pronounced as the experimentally observed turbulence – chemistry interaction increases. As such, the insensitivity of EMST can equally be interpreted as a model shortcoming [20]: the EMST model suffers from lack of local extinction with the applied chemistry model, regardless of the turbulence model applied. On the other hand, it is stressed once more that, with the EMST model, a statistically stationary solution could be obtained for flame HM3 using RSM, while this turned out to be impossible with the CD mixing model.

## 6 Discussion

The present study does not allow to rule out either of the micro-mixing models studied. Whereas one could think of quantification of errors for each of the four combinations (two turbulence model and two micro-mixing models) with respect to experimental data, such a

quantification would only be valid for the test cases under study and would also depend on the chemistry model applied.

The general observation is that the CD mixing model predicts local extinction more accurately than the EMST model, which always under-predicts local extinction with the applied chemistry model. This model draw-back has been described in general terms by Fox [20]: in the limit of infinitely fast one-step reaction, particles cannot evolve away from the flame sheet with EMST. Apparently, for the test cases under study, with EMST and with the applied chemistry model, particles do not evolve towards the inert mixing limit to the same extent as experimentally observed, regardless of the results in physical space. In that sense, CD performs better. On the other hand, the 'jumps' in composition space are inherently unphysical, there is a tendency towards over-prediction of local extinction with CD for the test cases under study, and no statistically stationary solution could be obtained with the better turbulence model. Thus, in this context, we consider it impossible to call either of the micro-mixing models generally superior.

## 7 Conclusions

The impact of the results in physical space on the micro-mixing model behavior in composition space has been investigated for a series of bluff-body stabilized non-premixed turbulent flames with strong turbulence-chemistry interaction. The strong sensitivity of the CD micro-mixing results has been illustrated and has been explained from its basic principle of pair-wise particle interactions between randomly chosen particles in a given cell. This sensitivity can be seen as an inherent draw-back of application of the CD micro-mixing model in test cases where the physical space results are not, or not sufficiently, known in advance.

Similarly, the robustness of the EMST micro-mixing behavior with respect to the physical space results, has been demonstrated. It has been explained by its localness principle in composition space. However, the robustness is at the same time a model draw-back: with the present chemistry model, the EMST model systematically suffers from lack of local extinction, regardless of the RANS turbulence model applied. Nevertheless, the robustness of the EMST can be very convenient during the initial stages of a simulation study, in which some turbulence model parameters are tuned to obtain good results for mean velocity, Reynolds stresses and mean conserved scalar. It can thus be recommended to use EMST as initial micro-mixing model choice and to possibly proceed to other candidate micro-mixing models once the turbulence model is fixed. This strategy relies on the rather weak impact of different mean density fields, implied by different mixing models, on the turbulent flow and mean mixture fraction results. This condition is satisfied for the bluff-body flames studied in this work.

**Acknowledgments** Part of the work has been financed by the Fund of Scientific Research – Flanders (Belgium) (FWO-Vlaanderen) through project G.0070.03, by the COMLIMANS program and by the Spanish MEC under Project ENE 2005-09190-C04-04/CON.

## References

1. Pope, S.B.: Prog. Energy Combust. Sci. **11**, 119–192 (1985)
2. Dally, B.B., Masri, A.R., Barlow, R.S., Fiechtner, G.J., Fletcher, D.F.: Combust. Flame **114**, 119–148 (1998)

3. Dally, B.B., Fletcher, D.F., Masri, A.R.: Combust. Theory Model **2**, 193–219 (1998)
4. Janicka, J., Kolbe, W, Kollman, W: J. Non-Equil. Thermodyn. **4**, 47–66 (1979)
5. Subramaniam, S., Pope, S.B: Combust. Flame **115**, 487–514 (1998)
6. Subramaniam, S, Pope, S.B.: Combust. Flame **117**(4), 732–754 (1999)
7. Liu, K., Pope, S.B., Caughey, D.A.: Combust. Flame **141**(1–2), 89–117 (2005)
8. Mitaria, S., Riley, J.J., Kosály, G.: Phys. Fluids **17**(047101), 1–15 (2005)
9. Ren, Z.Y., Pope, S.B.: Combust. Flame **136**(1–2), 208–216 (2204)
10. Cao, R.R., Pope, S.B.: Combust. Flame **143**, 450–470 (2005)
11. Merci, B., Roekaerts, D., Naud, B.: Combust. Flame **144**(3), 476–493 (2006)
12. Merci, B., Roekaerts, D., Naud, B., Pope, S.B.: Combust. Flame **146**(1–2), 109–130 (2006)
13. Li, G., Naud, B., Roekaerts, D.: Flow Turbul. Combust. **70**(1–4), 211–240 (2003)
14. Merci, B., Dick, E.: Int. J. Heat Mass Transfer **46**(3), 469–480 (2003)
15. Smooke, M.D., Giovangigli, V.: Lect. Notes Physics **384**, 1–47 (1991)
16. Pope, S.B.: Combust. Theory Model. **1**, 41–63 (1997)
17. Launder, B.E., Reece, G.J., Rodi, W.: J. Fluid Mech. **68**, 537–566 (1975)
18. Merci, B., Vierendeels, J., Dick, E., Roekaerts, D., Peeters, T.W.J.: Combust. Flame **126**(1–2), 1533–1556 (2001)
19. Merci, B., Dick, E., De Langhe, C.: Combust. Flame **131**(4) 465–468 (2002)
20. Fox, R.O.: Computational Models for Turbulent Reacting Flows, Cambridge University Press, Cambridge, UK (2003)
21. Bilger, R.W., Starner, S.H., Kee, R.J.: Combust. Flame **80**, 135–149 (1990)